

A general purpose model for the condensed phases of water: TIP4P/2005

J. L. F. Abascal^{a)} and C. Vega*Departamento de Química Física, Facultad de Ciencias Químicas, Universidad Complutense, 28040 Madrid, Spain*

(Received 29 July 2005; accepted 20 September 2005; published online 19 December 2005)

A potential model intended to be a general purpose model for the condensed phases of water is presented. TIP4P/2005 is a rigid four site model which consists of three fixed point charges and one Lennard-Jones center. The parametrization has been based on a fit of the temperature of maximum density (indirectly estimated from the melting point of hexagonal ice), the stability of several ice polymorphs and other commonly used target quantities. The calculated properties include a variety of thermodynamic properties of the liquid and solid phases, the phase diagram involving condensed phases, properties at melting and vaporization, dielectric constant, pair distribution function, and self-diffusion coefficient. These properties cover a temperature range from 123 to 573 K and pressures up to 40 000 bar. The model gives an impressive performance for this variety of properties and thermodynamic conditions. For example, it gives excellent predictions for the densities at 1 bar with a maximum density at 278 K and an averaged difference with experiment of 7×10^{-4} g/cm³. © 2005 American Institute of Physics. [DOI: 10.1063/1.2121687]

I. INTRODUCTION

Due to its role in biological and industrial processes, there is a great interest in an accurate knowledge of the molecular interactions in water. For this reason, a large number of potential models for water have been proposed in the past (see the reviews by Guillot¹ for an appraisal of the results for different models and by Finney² for a critical discussion of the interactions in water models; see also the Chaplin website³ containing updated information on water structure and behavior). Recent years have seen the proposal of new potential models or the reparametrization of the old ones.⁴⁻¹³ Computer simulation is computationally intensive, and many of the problems for which it may yield useful information are particularly demanding. The intrinsic complication of the simulated system (interaction with biomolecules), or the wide range of thermodynamic conditions (water in the Earth's crust or in other planets) or the timescale of the processes (nucleation, interfaces) makes it convenient to design general purpose potential models. These models should fulfil two conditions: Generality (to be useful for a large set of properties and a wide range of conditions) and simplicity (especially from a computational cost point of view). The latter prerequisite precludes (at present) the consideration of polarizable models even though it is well known that polarizability plays a fundamental role in the properties of water. In order to simplify the water potential we assume that, in a certain degree, polarization effects can be included in an averaged way in the model.

A crucial decision for the calculation of potential parameters is the choice of the quantities used to fit them. The set of properties should be as small as possible to facilitate the fitting but large enough to render the resulting potential predictive for the rest of properties. It is then important to select

quantities that discriminate the goodness of the potential models. In the past, most of the water models were designed to account for a reduced set of properties at ambient conditions. Quite successful potential models have been proposed. Many optimized models were essentially fitted using very similar experimental data. Thus, their predictions barely allow one to prefer one model to another. This is especially true in the case of two of the most common models, namely SPC/E¹⁴ and TIP4P.¹⁵ Recently, the availability of a greater computational power has enabled the accurate calculation of other properties which, in turn, allowed the proposal of new potentials^{5,9} or the reparametrization of the old ones.^{4,7,10}

One of the most interesting features of water is the existence of a density maximum for the low pressure isobars. At normal pressure the temperature of maximum density (T_{md}) is very close to 4 °C. The first report of the calculation of the T_{md} using computer simulation was made by Stillinger and Raman for the ST2 potential.¹⁶ Since then, a number of papers have appeared showing that some of the more usual water models (SPC/E,¹⁷⁻¹⁹ TIP4P¹⁵) exhibit a T_{md} but some others (SPC, TIP3P) apparently did not. Recently, these authors²⁰ have demonstrated that SPC and TIP3P also exhibit a T_{md} . Nevertheless, the maximum in density for the mentioned models occurs at temperatures from 182 K for TIP3P to 253 K for TIP4P, i.e., at least 24 deg below the experimental value. As the existence and location of the T_{md} is a challenge for any water potential model, there has been a recent interest to include this property in the fitting of the potential parameters.^{5,10} Moreover, Paschek has pointed out that a proper description of density effects is an important requirement for a water model for the correct description of the hydrophobic effects.²¹ This led him to conclude that a water model exhibiting a density maximum at the correct temperature is desirable.

A good model of water should also provide at least a reasonable description of the solid phases. The suggestion to

^{a)}Electronic mail: abascal@quim.ucm.es

use the properties of the ice polymorphs to test the effective pair potentials of water dates back more than two decades.^{22,23} Recent calculations^{24–27} of the phase diagram of water involving solid phases confirmed that this is as a severe test of effective water potentials. The TIP4P model reproduces qualitatively the phase diagram while the results for the SPC/E and TIP5P models are quite poor; for example, the stable phase at the normal melting point for the latter models is not the hexagonal ice (Ih) but ice II. Notice that the structural differences between the ice polymorphs involve a different degree of distortion of the hydrogen bond network. For instance, each water molecule in ice Ih is hydrogen-bonded to its four nearest neighbors in a nearly perfect tetrahedral coordination. The distance between nearest neighboring oxygen atoms is 2.75 Å. In ice II, the O–O–O angles range from 80° to 128° and the distances between nearest oxygen neighbours vary from 2.75 to 2.84 Å.²⁸ As a consequence, the ability of a potential model to deal with the stability of the different ice forms is indicative of its ability to reproduce the rich variety of hydrogen-bonded structures present in the different ice phases. The importance of this statement goes beyond the solid state. Liquid water also consists of a network of distorted hydrogen bonds. A test of effective water potentials using the properties of the liquid phase, gives only an indication of its ability to reproduce the “average” hydrogen bond. Of course, this is useful in many situations but it is not valid enough in problems where the details of the interaction with the water molecule are important as, for example, the interaction between water and biomolecules. This explains why models which perform well for liquid water may fail in the prediction of the relative stability of the ice polymorphs.

Unfortunately, both the determination of the phase diagram and the calculation of the T_{md} are computationally intensive. For this reason, these properties have been scarcely employed in the parametrization procedures. Recently, the authors have shown²⁶ that it is relatively easy to evaluate the shift in temperature (or pressure) of any coexistence line produced by a change in the potential parameters. The procedure, based on the integration of a generalized Clapeyron equation, allows one to include the information provided by the solid-liquid and solid-solid coexistence lines in the fitting of the potential parameters. In fact, the authors used the methodology to calculate the parameters of a simple potential model (TIP4P/Ice) specifically designed to reproduce as close as possible the phase diagram of ice.²⁷ It has also recently been observed²⁰ that the T_{md} and the melting temperature are closely related. For a number of potentials the difference between these two temperatures is around 25 K. More importantly, this difference does not depend on a small change in the potential parameters. In this way, the calculation of the shift in the melting temperature T_m due to changes in the potential parameters enables an approximate calculation of the T_{md} . The relationship between T_{md} and T_m can then be used to simplify the evaluation of the T_{md} in early stages of the fitting procedure as it can be roughly calculated from the melting temperature with a substantial saving in computer time.

In this work we incorporate the properties of several ice

forms and the T_{md} to more commonly employed quantities in order to parametrize a new potential model for water intended for a wide spectrum of properties and thermodynamic states. For reasons which become apparent later in this paper we opted to reparametrize the TIP4P functional form. Section II describes the simulation methodology. Section III presents the fitting procedure, and Sec. IV reports the results for the model. A final section discusses the main conclusions of this work.

II. THE SIMULATIONS

In TIP4P there is a single Lennard-Jones (LJ) interaction site at the oxygen and electrostatic charges at the hydrogens while the negative charge is placed in a site M along the bisector of the H–O–H angle and coplanar with the oxygen and hydrogens. In our simulations, the LJ potential was truncated at 8.5 Å. Standard long-range corrections to the LJ energy were added. The Ewald summation technique has been employed for the calculation of the long-range electrostatic forces. For the real space cutoff we also employed 8.5 Å. The screening parameter and the number of vectors in the reciprocal space considered was carefully selected for each phase. The sample size for water in the liquid state was 360 water molecules. The number of molecules for the different ice phases was chosen so as to fit at least twice the cut-off distance in each direction. Unless otherwise stated, the simulations were carried out using the Monte Carlo method at constant pressure and temperature (NpT). Isotropic NpT simulations are adequate for the liquid phase while anisotropic Monte Carlo simulations (Parrinello-Rahman-type)^{29,30} are required for the solid phases. For the calculation of the static dielectric constant and the self-diffusion coefficient we have used the molecular-dynamics package DLPOLY.³¹ The water molecules are treated as rigid bodies with orientations defined in terms of quaternions. A time step of 0.25 fs ensures energy conservation within a 0.05% in a 15 million steps run.

Recently, it has been demonstrated that the coexistence points of a given model may be accurately obtained from those of a different potential. The method is a generalization of the integration of the Clapeyron equation sometimes denoted as Gibbs-Duhem integration.^{32,33} A complete description of our implementation of the method can be found in Ref. 26. For completeness we sketch here a brief summary of this “Hamiltonian” Gibbs-Duhem integration. Let us write a given pair potential in terms of a reference potential as a function of a parameter λ

$$u = (1 - \lambda)u_{\text{ref}} + \lambda u_{\text{new}}, \quad (1)$$

when $\lambda=0$, $u=u_{\text{ref}}$ and for $\lambda=1$ it follows that $u=u_{\text{new}}$. We can use λ as a new intensive thermodynamic variable so that a change in the Gibbs free energy per particle is given by

$$dg = -s dT + v dp + x_g d\lambda. \quad (2)$$

It can be shown that the conjugate extensive thermodynamic variable x_g is

$$x_g = \frac{1}{N} \left\langle \frac{\partial U(\lambda)}{\partial \lambda} \right\rangle_{N,p,T,\lambda} \quad (3)$$

From this result, following the same steps leading to the classical Clapeyron equation, it is easy to write the generalized relationships

$$\frac{dT}{d\lambda} = \frac{\Delta x_g}{\Delta s} \quad (4)$$

and

$$\frac{dp}{d\lambda} = - \frac{\Delta x_g}{\Delta v} \quad (5)$$

The integration of these equations makes it possible to calculate the shift in the coexistence temperature (or pressure) produced by a change in the interaction potential at constant pressure (or temperature). We have checked that the Hamiltonian Gibbs-Duhem integration results are in very good agreement with the free energy calculations for the TIP4P and SPC/E models.²⁶ We have also shown that consistent results for the liquid-ice Ih coexistence temperature of TIP5P are obtained irrespective of the starting potential u_{ref} (TIP4P and SPC/E). Eight λ values were needed to go from SPC/E to TIP4P. The model investigated in this work is relatively similar to TIP4P, so that an integration using only three λ points has proven to be accurate enough for the transit from the TIP4P coexistence properties to those of the desired model. For the integration of the Hamiltonian Clapeyron equations a fourth-order Runge-Kutta method algorithm is employed. In the Runge-Kutta integration scheme, four different evaluations are required to go from a value of λ to the next one. About 90 000 cycles were performed for each λ value. The initial points for the starting model (TIP4P) were obtained from free energy calculations (see Ref. 24 for details).

III. A POTENTIAL MODEL FOR WATER

A. Fitting procedure

Formally, the first step of the fitting procedure is to make a Taylor expansion of the quantities to be fitted as a function of the parameters. Let us design the set of n parameters as $\xi = \{\xi_1, \dots, \xi_n\}$. Truncating the series at first order, we may write for a given property ψ

$$\psi \approx \psi^0 + \sum_{i=1,n} \frac{\partial \psi}{\partial \xi_i} (\xi_i - \xi_i^0), \quad (6)$$

where ξ_i denotes a particular parameter of the set ξ . The fit requires the knowledge of a selected set of m quantities for a starting model potential $\psi^0 = \psi(\xi^0)$ and the derivatives with respect to the parameters. In this way, the determination of the model parameters is done by a nonlinear fit of the selected set of properties that minimizes the square of the weighted deviations with respect to the experimental values

$$\sum_{j=1,m} w_j (\psi_j - \psi_j^{\text{exp}})^2 = \min. \quad (7)$$

The derivatives can be calculated numerically. A simple recipe uses the computed values of the quantity at two values of the parameter (symmetrically placed with respect to the starting parameter) while fixing the rest of the variables. Notice that, in this method, the properties of the starting potential are not used for the calculation of the derivatives, which is a waste of available information. On the other hand, the dependence of a quantity on the parameters is not necessarily linear. Thus, such parametrization procedure would be only approximate, and the final properties would differ from those predicted in the fit. Thus, we decided to simplify the calculation of the derivatives and to undertake the parametrization in two steps. For the calculation of the derivatives, we used only one point additional to that at which the property is initially known

$$\frac{\partial \psi}{\partial \xi_i} = \frac{\psi(\xi_i, \xi_{v \neq i}^0) - \psi(\xi^0)}{\xi_i - \xi_i^0}. \quad (8)$$

The calculated derivatives are somewhat less accurate than those obtained with the symmetric differentiation. In the second parametrization step, the intermediate potential is so close to the final result that both the linear approximation and the algorithm for computing the derivatives introduce negligible errors in the predicted quantities. Notice finally that the purpose of the fit is the calculation of the parameters. Thus, Eq. (6) is only used in the fitting procedure. Once the model parameters are known, the final properties of the new potential are obtained using standard simulation techniques. In other words, there are no approximations for the properties of the final model apart from those associated to the simulation protocol of each property.

B. Choice of the set of fitting properties

It is well known that it is not possible to fit the overall water properties with a single set of parameters. Otherwise, there would be no explanation for the vast number of water models proposed in the literature. One solution to the problem is to develop specialized potentials for a given set of properties and/or for a given range of temperatures and pressures. With this idea in mind, we have proposed the TIP4P/Ice model to be used in the studies of solid and amorphous water phases.²⁷ Our purpose in this paper is different. We intend to develop a potential model as general as possible. Obviously, the concept of ‘‘generality’’ is somewhat subjective so we should argue the criteria used to reach that goal.

Our analysis of the better performance of TIP4P in reproducing the low temperature phase diagram of water pointed undoubtedly to the placement of the negative charge apart of the oxygen atom in the direction of the hydrogens.²⁴ Despite the fact that SPC/E is a very successful potential in several aspects, it fails in the prediction of the phase diagram because its negative charge is located on the oxygen atom. This overstabilizes ice II which takes over a great part of the phase diagram. The phase diagram of SPC/E can not be improved unless the center of the negative charge is shifted

towards the hydrogens so the model would transform into a four-center model. Thus we decided to use TIP4P as a template for a new model. To prevent situations like those for SPC/E, it is convenient to include in the fit some of the coexistence lines involving ice II. Ice II competes with ices Ih and III and with liquid water. We have shown elsewhere²⁷ that it makes sense to fit the interval of temperatures at which ice III is stable at a given pressure. Our experience with TIP4P-like models indicates that a reduced stability of ice II not only increases the stability of ice III but also makes ice Ih the most stable form at ambient conditions. The range of temperatures for which ice III is stable has been computed as the difference between the coexistence temperature of ices II-III and that of liquid water-ice III at 3 kbar.

The reasons for including the T_{md} in the fitting procedure have been already discussed in the introduction. There, we also indicated that the melting temperature of ice Ih and the temperature of maximum density are not independent. The experimental difference at $p=1$ bar is 4 K (unless otherwise stated, we will refer to the values of T_m and T_{md} at normal pressure). For the most common water models the departure is considerably larger than this value. In particular, for models similar to TIP4P the T_{md} is 21–23 K above the melting point.²⁰ An estimation of $T_{md}-T_m$ for the potential obtained in the first stage of the fitting procedure (see above) also gives a value around 22 K. It is thus not possible to simultaneously fit both properties. Nevertheless, there are some factors which may account for some of the discrepancy between simulation and experiment. First, quantum effects must be relevant. In fact, for D₂O, $T_{md}-T_m$ is about 7 deg. For “classical” water (i.e., water in the limit of infinite molecular weight) the departures could well increase up to 10 K.^{1,16} Another important effect not included in the model that can affect differently the T_{md} and T_m is the polarizability. Notice that the water molecules have essentially the same environment and density in all the thermodynamic states around the T_{md} . Thus, the possible errors introduced by the substitution of a polarizable model by a model with fixed charges is similar at any temperature close to the T_{md} so this property is barely affected. (Incidentally, this is another reason to include the T_{md} in the fit of any model with fixed charges). On the contrary, the phases coexisting at the melting point are substantially different. Besides the structural differences, the change in density from ice Ih to liquid water is around a 10%. Thus, it seems that the use of a nonpolarizable model will distinctly affect each of the phases at equilibrium. The situation is similar to what happens in liquid water when compared to the gas phase but in a lesser extent. It seems that the effect of the neglect of the polarizability in the T_m should be larger than for the T_{md} . Because of these reasons we think that a water model should reproduce the temperature of maximum density as close as possible at the cost of a possible degradation in the predicted melting temperature. Notice finally that the melting temperature of TIP4P is 232 K, about forty degrees below the experimental value so there is room for a simultaneous improvement of both T_m and T_{md} .

The situation seen with $T_{md}-T_m$ also appears when we analyze the interdependence between the melting temperature and the enthalpy of vaporization $\Delta_v H$. For TIP4P-like

models, it is not possible to simultaneously fit the melting temperature of ice Ih and the enthalpy of vaporization.²⁷ The choice of a pair potential with a rigid geometry implies that the effect of the electrical polarization should be included in an averaged way. Thus, effective water potentials exhibit larger dipole moments than that of the isolated molecule. There is a growing acceptance of the idea that a self-energy correction¹⁴ should also be included if a comparison is made between the properties of the liquid state and the gas phase.¹ In fact, much of the reparametrization done for the TIP4P/Ew model¹⁰ is probably a consequence of the acceptance of this argument. The correction depends on the difference between the dipole moment of the model μ_l and that of the gas phase μ_g and may be approximated by

$$\Delta E_{\text{pol}} = (\mu_l - \mu_g)^2 / 2\alpha. \quad (9)$$

In this work we have also included the correction in the calculation of $\Delta_v H$. But despite the introduction of the self-polarization energy, it is still not possible to obtain a set of parameters (within the TIP4P functionality) producing at the same time good predictions for the enthalpy of vaporization and for the melting temperature of hexagonal ice. Interestingly, the correlation between T_m and $\Delta_v H$ goes in the opposite direction to the correlation between T_m and T_{md} . In other words, a perfect fit of $\Delta_v H$ implies a too low T_m . This reinforces our idea that a good prediction for the T_{md} will also produce a good balance between the deviations of T_m (always too low) and $\Delta_v H$ (too large) with respect to the experimental results. The dilemma posed by the fit of these three quantities would disappear (at least partially) by increasing the effective dipole moment of ice Ih. In such a case, the ice would gain stability and the melting temperature would shift towards higher temperatures. This observation is in agreement with recent calculations which indicate that the effective dipole moment of ice Ih is considerably greater than that of liquid water.^{11,34–36} As the T_{md} would remain unchanged, the final outcome would be a decrease of the difference between the melting temperature and the temperature of maximum density.

Another common property used in the fitting procedure is the liquid structure. Nevertheless, the procedure of extracting the site-site distribution functions from the measured scattering intensities has some ambiguities. In fact, only recently have converged the results obtained from x-ray and neutron scattering experiments.^{37,38} Thus, we believe that it is not (at present) a good target to parametrize the water potential. The previous statement does not contradict that reasonable agreement with the reported distribution functions should be produced by any acceptable water model. The choice of the rest of the properties included in our fitting procedure does not deserve particular comments. A common choice is the density of liquid water at room temperature. More input data is needed to avoid spurious effects when the number of fitting properties is the same as the number of parameters to be determined. We have tried with several properties observing that the final parameters are quite independent on the particular choice of these additional data. We finally selected the densities of ices II and V because its

TABLE I. Optimized parameters for the TIP4P/2005 model. The parameters of TIP4P (Ref. 15) and TIP4P/Ew (Ref. 10) are included for comparison.

Model	ϵ/k (K)	σ (Å)	q_H (e)	d_{OM} (Å)
TIP4P	78.0	3.154	0.520	0.150
TIP4P/Ew	81.9	3.16435	0.52422	0.125
TIP4P/2005	93.2	3.1589	0.5564	0.1546

simultaneous fit also seemed difficult (see Table I of Ref. 27). In summary, the set to be fitted consisted of six properties: The T_{md} (indirectly estimated from the melting point of ice Ih), the enthalpy of vaporization, the densities of liquid water at ambient conditions, of ice II at 123 K and 0 MPa, and of ice V at 223 K and 530 MPa, and, finally, the range of temperatures at which ice III is the thermodynamically stable ice at a pressure of 300 MPa.

C. The TIP4P/2005 model

Our aim is to construct a rigid model based in the the Bernal-Fowler geometry (which is essentially the TIP4P geometry) and functionality. There are four interaction sites. Three of them are placed at the oxygen and hydrogen atom positions, respectively. The other site, often called the M site, is coplanar with the O and H sites and is located at the bisector of the H–O–H angle. As in the original Bernal-Fowler and TIP4P models, we have fixed the O–H distance and H–O–H angle to the experimental values, 0.9572 Å and 104.52°, respectively. The total potential energy of the system is the sum of the pair interactions between molecules. The intermolecular pair potential has two contributions, a Lennard-Jones u_{LJ} term and an electrostatic interaction $u_{\text{electrostatic}}$. An important feature of the model is that the oxygen site carries no charge, but contributes to the the LJ term. The expression for the LJ interaction between two molecules is

$$u_{LJ} = 4\epsilon[(\sigma/r_{OO})^{12} - (\sigma/r_{OO})^6], \quad (10)$$

where r_{OO} is the distance between the oxygen sites of two molecules. Conversely, the H and M sites are charged, but do not contribute to the LJ term. The electrostatic potential between molecules i and j is then

$$u_{\text{electrostatic}} = \frac{e^2}{4\pi\epsilon_0} \sum_{a,b} \frac{q_a q_b}{r_{ab}}, \quad (11)$$

where e is the proton charge, ϵ_0 is the permittivity of vacuum, and a and b stands for the charged sites of molecules i and j , respectively. As a consequence of the molecular geometry and potential definitions, there are four unknown parameters to determine, namely, the strength ϵ and size σ of the LJ center, the hydrogen site charge (or the charge of the M site, $q_H = -q_M/2$), and the distance d_{OM} between the oxygen and the M site.

The two step procedure for the refinement of the potential model can be further simplified. This is because we may benefit from the knowledge of the properties of the model obtained in the first step of the parametrization of the TIP4P/Ice model. In this way the second parametrization step con-

TABLE II. Dipole moment and components of the quadrupole moment.

Model	μ^a	Q_{xx}^b	Q_{yy}	Q_{zz}
TIP4P	2.177	2.20	-2.09	-0.11
TIP4P/Ew	2.321	2.21	-2.11	-0.10
TIP4P/2005	2.305	2.36	-2.23	-0.13
Gas(expt.)	1.85	2.63	-2.50	-0.13

^aUnits are 10^{-18} esu cm.

^bUnits are 10^{-26} esu cm².

sisted in a fine tuning of the values of parameters using known data for both TIP4P and this intermediate model. The values of the optimized parameters for the TIP4P/2005 model are given in Table I.

The dipole moment and the components of the quadrupole tensor (referred to the center of mass) are presented in Table II. The resulting moments are approximately a 6% higher than those of TIP4P. Notice that opposite to the behavior of the effective dipole moment (which is larger for the rigid models than for an isolated molecule), the effective quadrupole tensor of TIP4P and TIP4P/2005 are smaller than the experimental one. Nevertheless, the quadrupole components for the TIP4P/2005 model are midway between those of TIP4P and of the gas phase. Interestingly, recent work indicates that a better agreement between a model and the experimental quadrupole moments leads to a considerable improvement in the properties of polarizable water models.^{39,40}

IV. RESULTS

A summary of the properties at ambient conditions is presented in Table III. The TIP4P/2005 model gives an excellent performance despite that our fit does not put special emphasis in this thermodynamic state. The model yields better predictions than the other models considered for most of the properties investigated. In following subsections we present a deeper investigation of the properties of the model.

A. Liquid densities at normal pressure

Table IV presents the numerical values of the liquid densities at $p=1$ bar. The number of cycles in the simulations were between 0.8×10^6 (high temperature states) and 1.5×10^6 (low temperatures). The estimated error, calculated as the 95% confidence interval varies from 0.001 g/cm³ at 370 K to 0.003 g/cm³ at 250 K. The dependence of the density with temperature is plotted in Fig. 1 together with the experimental data. The agreement is excellent at all the temperatures, no systematic drift is observed neither at low nor at high temperatures. Notice that most of the differences respect the experimental values is due to the noise of the simulation. We have fit the simulation densities to different polynomial expressions. A good choice that combines a relatively small number of coefficients, good statistics and absence of spurious effects in the predicted values and its derivatives is

TABLE III. Computed properties for liquid water at 298 K and 1 bar. Second and successive columns represent the values for the density ρ , isothermal compressibility κ_T , thermal expansion coefficient α_p , heat capacity at constant pressure C_p , heat of vaporization $\Delta_v H$, static dielectric constant ϵ , and self-diffusion coefficient D , respectively. $\Delta_v H$ for TIP4P/Ew and TIP4P/2005 include the self-polarization—Eq. (9). Other correction terms as given by Ref. 10 have been applied to C_p . In parentheses are the results of Eqs. (16) and (17) without any further correction. The results for TIP4P and TIP5P have been taken from Ref. 41 except the TIP4P dielectric constant and diffusion coefficient which come from Ref. 4. The results for TIP4P/Ew come from the original paper (Ref. 10).

Model	ρ (g/cm ³)	$10^5 \kappa_T$ (MPa ⁻¹)	$10^5 \alpha_p$ (K ⁻¹)	C_p (cal mol ⁻¹ K ⁻¹)	$\Delta_v H$ (kcal/mol)	ϵ	$10^9 D$ (m ² /s)
TIP4P	1.001	59	44	20	10.65	52	3.9
TIP5P	0.999	40.5	63	29	10.46	82	2.6
TIP4P/Ew	0.9954	48.1	33	19.2 (21.4)	10.58 (11.76)	63.4	2.44
TIP4P/2005	0.9979	46.5	28	18.9 (21.1)	10.89 (11.99)	60	2.08
Expt	0.9971	45.8	25.6	18.0	10.52	78.4	2.27

the expression $\rho = a + b/T + c/T^2 + d/T^3 + e/T^4 + f/T^5$. The coefficients of the fit are $a = 3.04516$, $b = -3873.33$, $c = 2.59696 \times 10^6$, $d = -8.2401 \times 10^8$, $e = 1.27848 \times 10^{11}$, and $f = -7.9149 \times 10^{12}$. The resulting expression gives a maximum density of $\rho = 1.0005$ g/cm³ at 278 K, with a 95% confidence interval of ± 3 K. The average of the absolute differences of the polynomial fit results respect to the experimental data is only 7×10^{-4} g/cm³ which is lower than the statistical error in the simulations.

The TIP4P/Ew results are also shown in Fig. 1. Indeed, these are also excellent predictions but not to the extent of our model. The TIP4P/Ew slightly overestimates the density at low temperatures and underestimates it at high temperatures. As a consequence, the T_{md} moves slightly towards lower temperatures (Horn *et al.*¹⁰ report a value of 274 K). It should be recalled that the TIP5P model, designed to reproduce the T_{md} , predicts a too strong temperature dependence. For instance, at $T = 75$ °C the TIP5P model underestimates the experimental density by $\approx 2.5\%$ ⁵ (the largest deviation from experiment of our fitted densities is less than a 0.2%). Besides, these results for TIP5P were obtained using a simple spherical cutoff for the electrostatic forces. It is known that the use of Ewald sums decreases the densities and shifts the T_{md} towards higher temperatures. Using a

TABLE IV. Liquid densities (g/cm³) at $p = 1$ bar.

T/K	TIP4P/2005	Expt.
250	0.9908	0.9913
260	0.9965	0.9970
270	1.0010	0.9995
280	0.9994	0.9999
290	0.9993	0.9988
298	0.9979	0.9971
300	0.9965	0.9965
315	0.9913	0.9915
330	0.9841	0.9848
340	0.9776	0.9795
350	0.9713	0.9737
360	0.9668	0.9674
370	0.9585	0.9606

proper treatment of long-range forces, several authors agree in a value of $\rho = 0.983$ g/cm³ for TIP5P at 298 K and normal pressure^{20,21,42,43} and a T_{md} around 285 K.^{20,42} These results are very poor when compared to those for TIP4P/Ew and TIP4P/2005.

B. Expansivity

The thermal expansion coefficient, α_p , is defined as

$$\alpha_p = - \frac{1}{V} \left(\frac{\partial V}{\partial T} \right)_p. \quad (12)$$

The above expression indicates that α_p can be simply computed by analytic differentiation of the polynomial fit of the densities at $p = 1$ bar reported above. The calculated values are plotted in Fig. 2 together with the experimental data. The values for TIP4P/Ew, taken from the original work,¹⁰ are also included for comparison. As expected from our comments in the preceding subsection, the TIP4P/2005 model results are

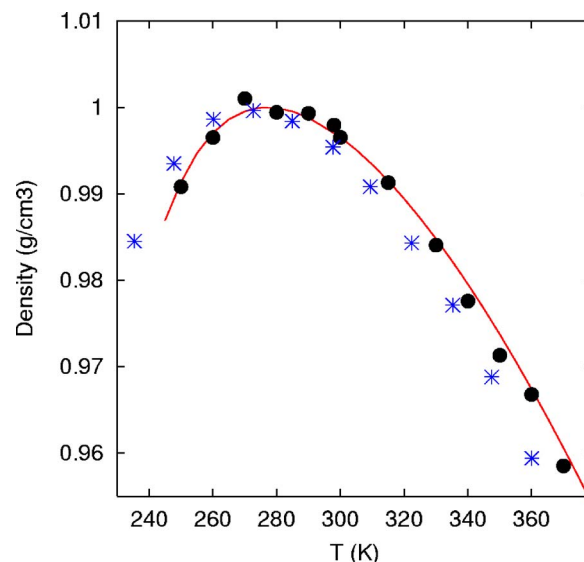


FIG. 1. Densities of the TIP4P/2005 model (circles) at $p = 1$ bar compared to the reported values for TIP4P/Ew (Ref. 10) (stars) and experimental data (full line).

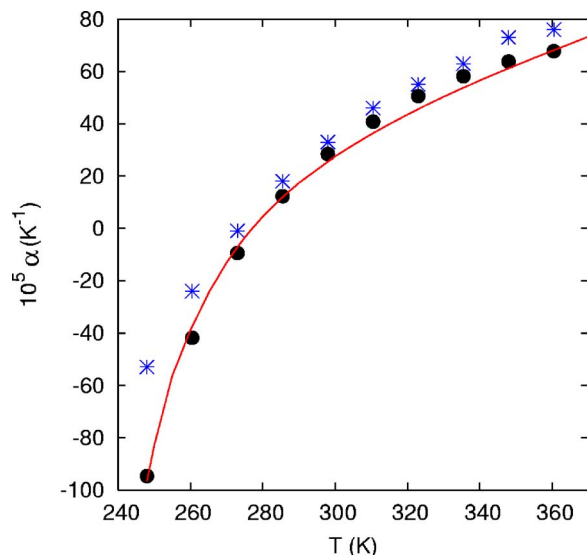


FIG. 2. Variation with temperature of the thermal expansion coefficient at $p=1$ bar. Symbols are the simulation results (stars: TIP4P/Ew; circles: TIP4P/2005). The full line represents the experimental data.

very accurate while the deviations for the TIP4P/Ew model are significant (about 45% at $T=248$ K and 18% at 373 K).

C. Compressibility

The isothermal compressibility is defined as

$$\kappa_T = -\frac{1}{V} \left(\frac{\partial V}{\partial p} \right)_T \quad (13)$$

The variation of the volume with pressure is quite smooth so a polynomial fit again seems to be adequate. In fact, the volumes in the interval -200 to 1250 bar can be accurately fitted to a second-order polynomial. Nevertheless, a fit of the experimental results in the same range indicate that the second degree polynomial is acceptable in the central part of the interval but that a third-order could be required for the compressibilities at $p=1$ bar and $p=1000$ bar. The uncertainty of the simulated volumes (about 0.15% using 1×10^6 cycles) does not allow for a third-order polynomial fit. Thus, for these points we made use also of the fluctuation formula

$$\kappa_T = \frac{\langle V^2 \rangle - \langle V \rangle^2}{kT \langle V \rangle} \quad (14)$$

The latter computations were obtained in 10 million steps of a molecular-dynamics simulation. The uncertainty of the calculated compressibilities is about 1×10^{-5} MPa^{-1} for $p=1$ bar and 0.7×10^{-5} for $p=1000$ bar. The dependence of κ_T with pressure is plotted in Fig. 3. Again, the predictions of the TIP4P/2005 model are in excellent agreement with experiment. Moreover the slope of the experimental and the TIP4P/2005 curves are similar. In fact, very costly simulations would be required to give a more precise answer to the extent of the differences between the model and the experiment.

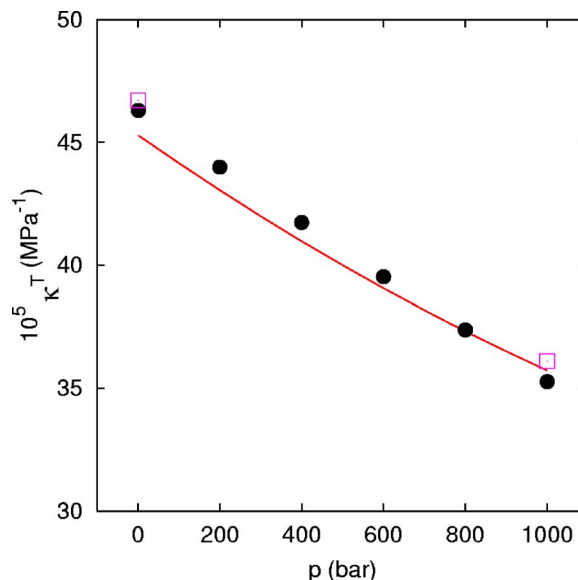


FIG. 3. Variation with pressure of the isothermal compressibility at 298 K. Symbols are the simulation results (squares: Fluctuation formula; circles: Using the derivative of the polynomial fit of V vs p). The full line represents the experimental data.

D. Equation of state at high pressures

The results presented above referred to thermodynamic states not too far from ambient conditions. There, it has been shown that TIP4P/2005 gives remarkable predictions not only for the equation of state but also for derived properties. Figure 4 shows the densities for two isotherms at relatively high temperatures (473 and 573 K) up to 40 000 bar. The simulation results agree very well with recent experimental data.⁴⁴ The departures increase with pressure but are always quite small. The maximum deviation is 0.45% for $T=473$ K, $p=30$ 000 bar and 0.9% at $T=573$ K, $p=40$ 000 bar.

E. Densities of the ice polymorphs

The densities of several ice forms are shown in Table V. Once again the TIP4P/2005 model gives excellent predic-

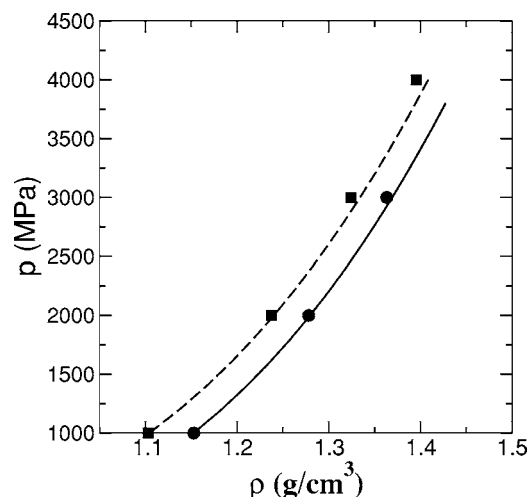


FIG. 4. Equation of state at high pressures as obtained from experiment and from the simulations of this work for the TIP4P/2005 model. Lines: Experimental results. Solid line, $T=473$ K; dashed line, $T=573$ K. Symbols: Simulation results. Circles, $T=473$ K; squares, $T=573$ K.

TABLE V. Densities (g/cm^3) of several ice forms at the temperature and pressure indicated. The last two rows are the mean value of the (signed) deviations from the experimental data $\bar{d} = \sum d/N$ ($d = \rho - \rho_{\text{exp}}$), and $\sigma_N = \sqrt{\sum d^2/N}$. The experimental data are taken from Ref. 45.

Ice	T/K	p/MPa	TIP4P/2005	Expt.
Ih	250	0	0.921	0.920
Ic	78	0	0.944	0.931
II	123	0	1.199	1.170
III	250	280	1.160	1.165
IV	110	0	1.293	1.272
V	223	530	1.272	1.283
VI	225	1100	1.380	1.373
IX	165	0.28	1.190	1.194
XI	5	0	0.954	0.934
XII	260	0.5	1.296	1.292
\bar{d}			0.007	
σ_N			0.014	

tions. It is a common feature that simple rigid models overestimate the ice densities (TIP4P/Ice is the exception to the rule). However, for the present model, the departures from experiment are quite small. The signed mean deviation is only $0.007 \text{ g}/\text{cm}^3$ to be compared with the reported values 0.070, 0.029, 0.028, 0.023 for TIP5P, SPC/E, TIP4P, and TIP4P/Ew, respectively.²⁷ Despite the fact that the densities of ices II and ice V were included in fitting set it was still not possible to improve the density of the former without deteriorating the prediction for the latter. In fact, as for all the models investigated until now, ice II gives the largest positive deviation from experiment while ice V gives the smallest deviation reaching a negative value for TIP4P/2005. Figure 5 represents the departures of the densities of different models with respect to the experimental values. This plot gives a graphical picture of the same type of information given by the mean deviations above reported.

There is another point which deserves a comment. Notice that the ordering of the deviations is essentially the same for all the models. In fact, to represent the results for the different polymorphs, we have followed the same sequence for all the models (that of TIP4P). As can be seen

in the figure, the amplitude of the deviations change from one model to other but the general behavior is the same (even in the case of TIP4P/Ice where signed mean deviation is negative).

F. Melting properties

The melting properties of ice Ih at $p=1$ bar are given in Table VI. The melting temperature is 252.1 K, about 20° below the experimental value. Leaving aside the TIP4P/Ice model (specifically designed to account for the properties of the solid amorphous water phases), the TIP4P/2005 model gives the most balanced predictions. Besides, the slope of the p - T coexistence line is in excellent agreement with the experiment which suggests good predictions also for the liquid water-ice Ih coexistence line. Notice that TIP5P predicts the melting temperature of ice Ih with a great accuracy, but it fails completely in the prediction of other melting properties, especially the volume change and the slope of the coexistence line as a consequence. This indicates that the TIP5P melting points differ noticeably from experiment at higher pressures. Moreover, it is to be stressed that for TIP5P it is ice II—not ice Ih—the thermodynamically stable phase at $p=1$ bar. Hence the melting temperature of the TIP5P model should be that of ice II (the stable phase at $p=1$ bar) which is ~ 283 K. Notice finally that the six-center model of Nada and van der Eerden⁹ provides an excellent estimate for the melting properties. Unfortunately, other properties for this model remain to be thoroughly checked.

G. Phase diagram

Figure 6(a) shows the dense region (up to moderately high pressures) of the phase diagram as computed for the TIP4P/2005 model. Only the stable phases in real water have been considered for the calculations. TIP4P/2005 improves the predictions of TIP4P (see Ref. 24) and gives a semiquantitative description of the coexistence between the different ice polymorphs. In fact, a slight shift in T and p (about

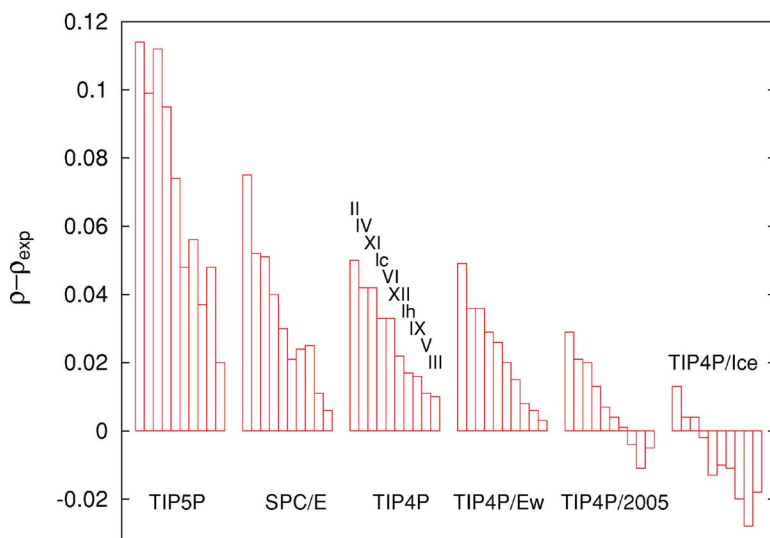


FIG. 5. Deviation from experiment of the ice densities (in g/cm^3) for different water models. The results are grouped according to the model. Within each group the results for the different ice polymorphs appears always in the same sequence (labeled only for TIP4P).

TABLE VI. Melting properties of ice Ih at $p=1$ bar for different models. T_m is the melting temperature; ρ_l and ρ_{Ih} , the densities of liquid water and ice; H_l and H_{Ih} , the corresponding enthalpies (the $3RT$ term arising from the translational and rotational kinetics terms is not included); ΔH_m , the melting enthalpy; and dp/dT , the slope of the coexistence curve. Data taken from Ref. 26 except for TIP4P/Ice (Ref. 27) and TIP4P/2005 (this work).

Model	SPC/E	TIP4P	TIP4P/Ew	TIP5P	TIP4P/Ice	TIP4P/2005	Expt
T_m (K)	215.0	232.0	245.5	273.9	272.2	252.1	273.15
ρ_l (g/cm ³)	1.011	1.002	0.992	0.987	0.985	0.993	0.999
ρ_{Ih} (g/cm ³)	0.950	0.940	0.936	0.967	0.906	0.921	0.917
H_l (kcal/mol)	-12.49	-10.98	-12.02	-10.33	-13.31	-12.17	
H_{Ih} (kcal/mol)	-13.23	-12.03	-13.07	-12.08	-14.60	-13.33	
ΔH_m (kcal/mol)	0.74	1.05	1.05	1.75	1.29	1.16	1.44
dp/dT (bar/K)	-126	-160	-164	-708	-120	-135	-137

20–30 deg and 100 MPa) to the TIP4P/2005 phase diagram would put it in perfect agreement with the experimental one. This is in strong contrast with the predictions of TIP5P and TIP4P/Ew. The results for TIP5P—see Ref. 26—are quite poor: Ice Ih is stable only at negative pressures and the slope of the liquid-ice Ih curve is positive in that region. This is because the model overestimates the stability of ice II. In

fact, ices III and V are also metastable phases for TIP5P. The situation for TIP4P/Ew is less dramatic but it is still not satisfactory. Its phase diagram is shown in Fig. 6(b). Again, ice II takes over the region of moderately high pressures. As a result, ice III is metastable and the interval of stability of ice V is reduced to a marginal range of temperatures and pressures.

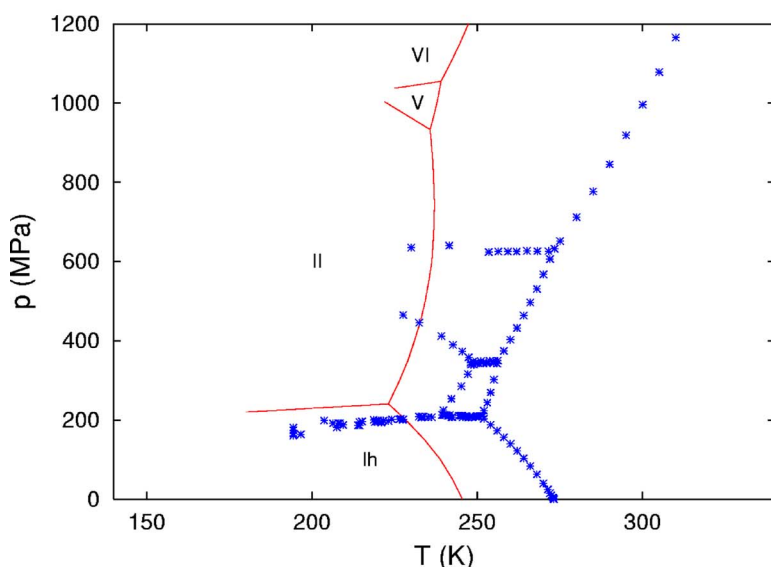
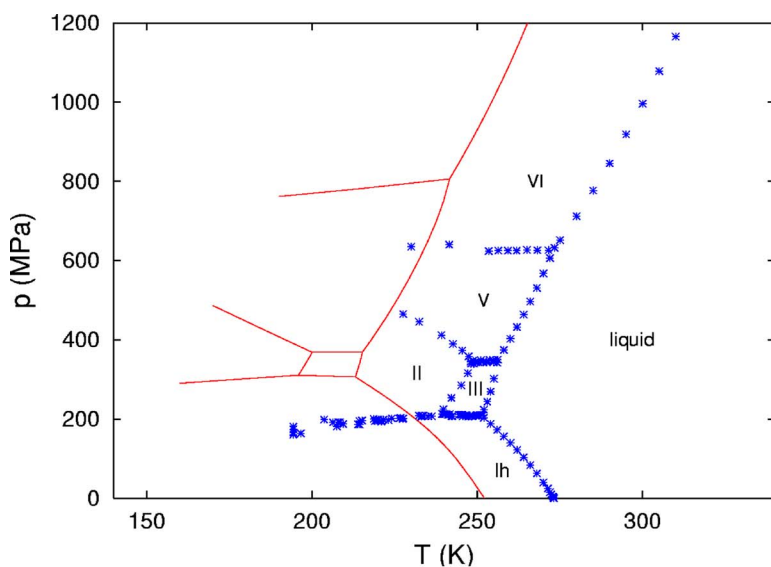


FIG. 6. Phase diagram of TIP4P/2005 (top) and TIP4P/Ew (bottom). The stars are the experimental results and the full lines represent the simulation values.

H. Enthalpy of vaporization

By definition, the enthalpy of vaporization is

$$\Delta_v H = H_{\text{gas}} - H_{\text{liquid}}. \quad (15)$$

At low pressures the gas may be considered ideal and gives a negligible contribution to the internal energy. Besides, its volume may be calculated from the perfect gases equation. In this way, the enthalpy of vaporization may be approximated by

$$\Delta_v H = -U_{\text{liquid}} - pV_{\text{liquid}} + RT. \quad (16)$$

We have already mentioned in the introduction that the above equation should be corrected to take into account the self-polarization term—Eq. (9)—arising from the difference between the dipole moment of the gas and the effective dipole moment of the liquid. Horn *et al.*¹⁰ have proposed a number of additional corrections in order to account for vibrational and nonideal gas effects. The polarization term depends on the effective dipole moment of the particular water model but the other correction terms are small and should be quite similar for TIP4P-like potentials. Because of this, and also to make a consistent comparison with TIP4P/Ew, the result for the enthalpy of vaporization reported in Table III include the correction term. The final result for TIP4P/2005 is slightly high when compared to the experiment even after the addition of the correction term. It has been argued by Guillot (Ref. 46) that it is more judicious to compare the result of a classical simulation with the value of $\Delta_v H$ expected for an hypothetical *classical* water. The value -11.0 kcal/mol is recommended as the limiting value of H₂O (10.52 kcal/mol), D₂O (10.87 kcal/mol), and T₂O (10.93 kcal/mol). Our result lies between this recommended value and the experimental one.

I. Heat capacity

The heat capacity at constant pressure is defined as

$$C_p = \left(\frac{\partial H}{\partial T} \right)_p. \quad (17)$$

In order to compute C_p we have calculated the enthalpy including the corrections commented in the above subsection. Then, we fitted the values of the enthalpy to a fifth-order polynomial and differentiated it with respect to temperature to obtain C_p at several temperatures. TIP5P gives the largest deviations from experiment while the predictions of TIP4P, TIP4P/Ew and TIP4P/2005 are similar (though slightly better for TIP4P/2005). As shown in Fig. 7 TIP4P/Ew and TIP4P/2005 give a semiquantitative description of the dependence of C_p with temperature at normal pressure. The deviation is about 10% at 273 K (10.9% and 9.6%, respectively, for TIP4P/Ew and TIP4P/2005) and decreases upon increasing the temperature, at 335.5 K the difference is only of 3.5%. TIP5P predicts too large values for C_p together with a strong dependence on T . The deviations respect the experimental values are: Over a 100% at -12.5 °C, around 60% at 25 °C and about 40% at -75 °C.

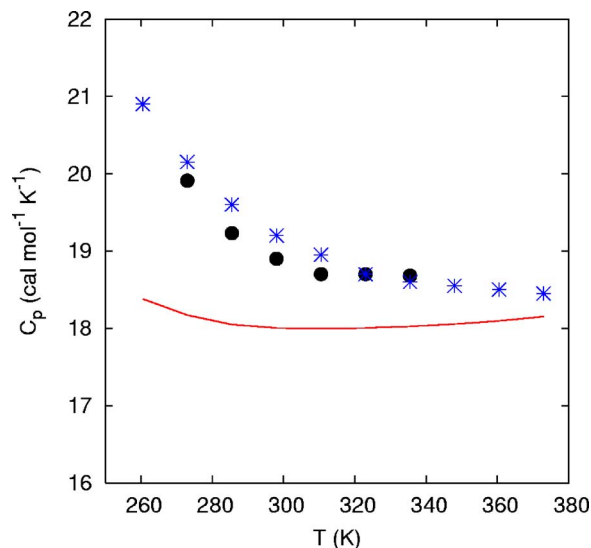


FIG. 7. Isobaric heat capacity as a function of temperature. Symbols are the simulation results (stars: TIP4P/Ew; circles: TIP4P/2005). The full line represents the experimental data.

J. Static dielectric constant

The equation for the calculation of the static dielectric constant in a simulation using Ewald sums with conducting boundary conditions reads⁴⁷

$$\varepsilon = 1 + \frac{4\pi}{3kTV} (\langle \mathbf{M}^2 \rangle - \langle \mathbf{M} \rangle \langle \mathbf{M} \rangle). \quad (18)$$

We have computed ε from a 15 million steps NVE molecular dynamics simulation representing 3.75 ns. From the drift in the curve we estimate the uncertainty to be about 4. The final result is $\varepsilon=62$ for a mean temperature of $T=291.3$ K. To simplify the comparison with other results in Table III, it is interesting to extrapolate this value at 298 K. Assuming that the dependence of ε on T is the experimental one, the value at 298 K would be about 60. A similar value has been obtained in a shorter (1.5 ns) simulation run with the sample size increased to 530 molecules and a cutoff of 12 Å. Notice that the increase of the TIP4P/2005 charges with respect to TIP4P provokes an increase in the dielectric constant which approaches the experimental value. However, it is slightly lower than that of TIP4P/Ew.

K. Diffusivity

For the calculation of the self-diffusion coefficient we used the Einstein equation

$$6Dt = \lim_{t \rightarrow \infty} \langle |\mathbf{r}_i(t) - \mathbf{r}_i(0)|^2 \rangle, \quad (19)$$

where $\mathbf{r}_i(t)$ represents the position of particle i at time t . The molecular dynamics runs used for the calculation of the dielectric constant have been used for D . The result for the 360 molecules sample (3.75 ns) is $1.74 \pm 0.05 \times 10^{-9}$ m²/s for a temperature of 291.3 K. As the experimental values of the diffusion coefficient, D_{exp} , shows a strong dependence on temperature, it is necessary to find the experimental value at the simulation temperature. By interpolating at $T=291.3$ we find $D_{\text{exp}}=1.87 \times 10^{-9}$ m²/s⁴⁸ and $D_{\text{exp}}=1.93 \times 10^{-9}$ m²/s.⁴⁹

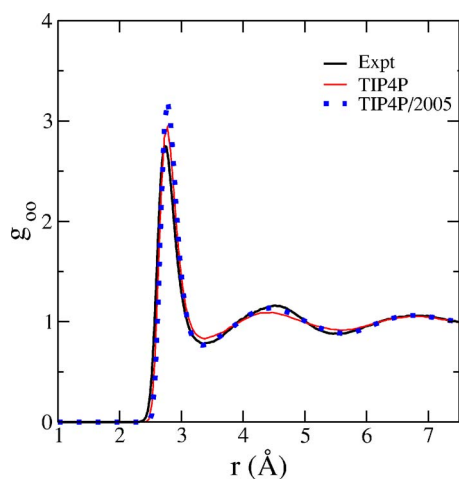


FIG. 8. Oxygen-oxygen correlation function at 298 K. Thick (black) line: Experimental data (Ref. 38); thin (red) line: TIP4P; dotted (blue) line: TIP4P/2005.

The result of the molecular dynamics run using 530 molecules is $2.00 \times 10^{-9} \text{ m}^2/\text{s}$ for a temperature of 297.1 K. In order to compare with other results at 298 K we have used the experimental dependence on temperature. The results extrapolated at 298.15 K are 2.10×10^{-9} and $2.06 \times 10^{-9} \text{ m}^2/\text{s}$ for the systems with 360 and 530 molecules, respectively. The difference is within the estimated error so the dependence on the sample size (if any) is quite small. This is probably due to the fact that the effect of increasing the number of molecules is usually opposite to that of increasing the cutoff radius (see Table III of Ref. 4). As seen in Table III the TIP4P/2005 model improves the predictions of TIP4P and TIP5P and are of similar quality as TIP4P/Ew (the value given in Ref. 10 has been extrapolated at 298.15 K). In fact both models yield results which are almost equidistant from the values $2.3 \times 10^{-9} \text{ m}^2/\text{s}$ reported by Mills and by Krynicki *et al.*^{49,50} and $2.23 \times 10^{-9} \text{ m}^2/\text{s}$ reported by Gillen *et al.*⁴⁸

L. Liquid structure

The oxygen-oxygen correlation function, $g_{\text{OO}}(r)$ is represented in Fig. 8. The agreement with the experimental curve is quite satisfactory though there are some discrepancies in the height of the first peak. However, from the first minimum, the TIP4P/2005 results are very close to the experimental data and improves substantially the predictions of TIP4P.

V. CONCLUDING REMARKS

In this paper we have presented the results for a new potential model intended to be a general purpose model for the condensed phases of water. The calculated properties include a number of thermodynamic properties of the solid and liquid phases as well as several other properties of liquid.⁵¹ From the point of view of the thermodynamic conditions, the simulations covered a temperature range from 123 to 573 K and pressures up to 40 000 bar. In summary, we have checked the model for a rather complete set of water properties and an unusually wide range of states. The model gives

an impressive performance for this variety of properties and thermodynamic conditions. The results are clearly better than those for its predecessor TIP4P. The comparison is also satisfactory with last generation potentials as TIP4P/Ew and TIP5P. The latter model seems to reproduce very well a limited set of properties but the agreement with experiment for some of them (melting point and T_{md}) deteriorate noticeably when the electrostatic interactions are properly calculated. Besides, TIP5P gives poor predictions for other properties (compressibility, expansivity, heat capacity, dense region of the phase diagram, densities of ices).

The performance of TIP4P/Ew is excellent for many properties. But the poor prediction of the phase diagram indicates that it does not account for the distortions in the hydrogen bond network. A possible explanation is the low value of its quadrupole moments which is compensated with a larger dipole. In this way the averaged effect of the electrostatic interactions may be correct but the angular dependence is probably not so good. A deeper investigation of the reasons of the overstability of ice II for this model could throw some light on this point. It is also to be pointed out that the differences in the structural predictions of several models for ice II are considerably larger than for other ice forms (see Ref. 52). Notice finally that—apart of this serious failure of TIP4P/Ew—, for most of the properties investigated, the predictions of TIP4P/2005 are more accurate. In fact, the only property for which TIP4P/Ew performs clearly better is the enthalpy of vaporization. The TIP4P/Ew result for the static dielectric constant is slightly better than that for TIP4P/2005 while both models perform similarly for the self-diffusion coefficient. For the rest of properties (densities at normal pressure, T_{md} , expansivity, compressibility, densities of the ice polymorphs, melting properties, phase diagram and heat capacity) the results of TIP4P/2005 are clearly better than those for TIP4P/Ew.

An important conclusion of our study is the interdependence of many of the water properties in reparametrized TIP4P potentials. An attempt to match the experimental ice Ih melting temperature (as done in TIP4P/Ice²⁷) implies too large a vaporization enthalpy and a too high T_{md} . Conversely, as the original TIP4P model was designed to match the vaporization enthalpy, their predictions for T_m and T_{md} are too low.⁵³ On the other hand, since TIP4P/2005 has been designed to match the T_{md} , it yields a slightly low melting temperature and a somewhat large vaporization enthalpy. It is clear that there is room for dedicated potentials, i.e., for models that reproduce very well the water behavior for a particular set of properties and give an acceptable account of the rest of properties. But there are important applications (biomolecular simulations could be the paradigm) where this it is not possible because the comparison with experiment is not trivial. For those applications a “general purpose” model is needed. Due to the disparity of properties it is not possible to provide an unequivocal assessment of the quality of different models. A critical discussion of the quality of the different results is then necessary.

The overall performance of TIP4P/Ew and TIP4P/2005 (especially when compared with the original TIP4P) strongly supports the need of a self-energy term which is at the origin

of SPC/E.¹⁴ Other quantum effects could be incorporated in path integral simulations. Admittedly, we wanted to propose a model that reproduces the experimental properties of water within a classical framework. But, given the limitations of the model, it seems important that the deviations from experiment are at least compatible with the neglected effects. This is why we find acceptable the small deviations in the enthalpy of vaporization of TIP4P/2005. On the other hand, it has been widely commented that a better agreement for $\Delta_v H$ implies a low value for the melting temperature. It is clear that the most important applications of the water simulations involve condensed phases including amorphous water.⁵⁴⁻⁵⁶ Thus, nowadays, the prediction of a single valued property involving the vapor phase cannot be as important as in the past. Probably, the melting properties are more indicative of the reliability of the potential model. However, melting poses a problem similar to vaporization: The water environment differs noticeably in both phases at coexistence. Again, heuristic arguments indicate that the corrections due to a higher dipole moment in the solid phase would probably move the melting temperature towards the experimental results. The above arguments apply only to TIP4P-like potentials. For other types of potentials as TIP5P, the apparent difference between melting temperature and the T_{md} is only 11 K²⁰ although the reported T_m is for ice Ih which is a metastable phase in those conditions. In summary, TIP4P/2005 gives an excellent performance for most of the properties investigated and the departures from experiment for other properties are well balanced and justified. It seems then a reliable water potential within the limitations inherent to a four-site rigid potential model with fixed charges.

ACKNOWLEDGMENTS

This research has been funded by project Nos. FIS2004-06227-C02-02 and FIS2004-02954-C03-02 of the Spanish DGI (Dirección General de Investigación). We would like to thank L. G. MacDowell for stimulating discussions and C. McBride for technical help.

¹B. Guillot, *J. Mol. Liq.* **101**, 219 (2002).

²J. L. Finney, *J. Mol. Liq.* **90**, 303 (2001).

³M. Chaplin, <http://www.lsbu.ac.uk/water>.

⁴D. van der Spoel, P. J. van Maaren, and H. J. C. Berendsen, *J. Chem. Phys.* **108**, 10220 (1998).

⁵M. W. Mahoney and W. L. Jorgensen, *J. Chem. Phys.* **112**, 8910 (2000).

⁶C. J. Burnham and S. S. Xantheas, *J. Chem. Phys.* **116**, 1479 (2002).

⁷A. Glättli, X. Daura, and W. van Gunsteren, *J. Chem. Phys.* **116**, 9811 (2002).

⁸H. Yu, T. Hansson, and W. F. van Gunsteren, *J. Chem. Phys.* **118**, 221 (2003).

⁹H. Nada and J. P. J. M. van der Eerden, *J. Chem. Phys.* **118**, 7401 (2003).

¹⁰H. W. Horn, W. C. Swope, J. W. Pitera, J. D. Madura, T. J. Dick, G. L. Hura, and T. Head-Gordon, *J. Chem. Phys.* **120**, 9665 (2004).

¹¹H. Saint-Martin, B. Hess, and H. J. C. Berendsen, *J. Chem. Phys.* **120**, 11133 (2004).

¹²S. W. Rick, *J. Chem. Phys.* **120**, 6085 (2004).

¹³L. R. Olano and S. W. Rick, *J. Comput. Chem.* **26**, 699 (2005).

¹⁴H. J. C. Berendsen, J. R. Grigera, and T. P. Straatsma, *J. Phys. Chem.* **91**, 6269 (1987).

¹⁵W. L. Jorgensen, J. Chandrasekhar, J. D. Madura, R. W. Impey, and M. L. Klein, *J. Chem. Phys.* **79**, 926 (1983).

¹⁶F. H. Stillinger and A. Rahman, *J. Chem. Phys.* **60**, 1545 (1974).

¹⁷L. A. Báez and P. Clancy, *J. Chem. Phys.* **101**, 9837 (1994).

¹⁸S. Harrington, P. H. Poole, F. Sciortino, and H. E. Stanley, *J. Chem. Phys.* **107**, 7443 (1997).

¹⁹T. Bryk and A. D. J. Haymet, *Mol. Simul.* **30**, 131 (2004).

²⁰C. Vega and J. L. F. Abascal, *J. Chem. Phys.* **123**, 144504 (2005).

²¹D. Paschek, *J. Chem. Phys.* **120**, 6674 (2004).

²²M. D. Morse and S. A. Rice, *J. Chem. Phys.* **76**, 650 (1982).

²³J. L. Finney, J. E. Quinn, and J. O. Baum, in *Water Science Reviews 1*, edited by F. Franks (Cambridge University Press, Cambridge, 1985).

²⁴E. Sanz, C. Vega, J. L. F. Abascal, and L. G. MacDowell, *Phys. Rev. Lett.* **92**, 255701 (2004).

²⁵E. Sanz, C. Vega, J. L. F. Abascal, and L. G. MacDowell, *J. Chem. Phys.* **121**, 1165 (2004).

²⁶C. Vega, E. Sanz, and J. L. F. Abascal, *J. Chem. Phys.* **122**, 114507 (2005).

²⁷J. L. F. Abascal, E. Sanz, R. G. Fernández, and C. Vega, *J. Chem. Phys.* **122**, 234511 (2005).

²⁸B. Kamb, *Acta Crystallogr.* **17**, 1437 (1964).

²⁹M. Parrinello and A. Rahman, *J. Appl. Phys.* **52**, 7182 (1981).

³⁰S. Yashonath and C. N. R. Rao, *Mol. Phys.* **54**, 245 (1985).

³¹W. Smith, M. Leslie, and T. R. Forrester, *J. Mol. Graphics* **14**, 136 (1996).

³²D. A. Kofke, *Mol. Phys.* **78**, 1331 (1993).

³³D. A. Kofke, *J. Chem. Phys.* **98**, 4149 (1993).

³⁴E. R. Batista, S. S. Xantheas, and H. Jönsson, *J. Chem. Phys.* **109**, 4546 (1998).

³⁵E. R. Batista, S. S. Xantheas, and H. Jönsson, *J. Chem. Phys.* **111**, 6011 (1999).

³⁶S. W. Rick, *J. Chem. Phys.* **114**, 2276 (2001).

³⁷G. Hura, J. M. Sorenson, R. M. Glaesera, and T. Head-Gordon, *J. Chem. Phys.* **113**, 9140 (2000).

³⁸A. K. Soper, *J. Chem. Phys.* **258**, 121 (2000).

³⁹H. Yu and W. F. van Gunsteren, *J. Chem. Phys.* **121**, 9549 (2004).

⁴⁰P. Paricaud, M. Předota, A. A. Chialvo, and P. T. Cummings, *J. Chem. Phys.* **122**, 244511 (2005).

⁴¹W. L. Jorgensen and J. Tirado-Rives, *Proc. Natl. Acad. Sci. U.S.A.* **102**, 6665 (2005).

⁴²M. Lísal, J. Kolafa, and I. Nezbeda, *J. Chem. Phys.* **117**, 8892 (2002).

⁴³Z. G. Zhang and Z. Duan, *Phys. Earth Planet. Inter.* **149**, 335 (2005).

⁴⁴E. H. Abramson and J. M. Brown, *Geochim. Cosmochim. Acta* **68**, 1827 (2004).

⁴⁵V. F. Petrenko and R. W. Whitworth, *Physics of Ice* (Oxford University Press, Oxford, 1999).

⁴⁶B. Guillot and Y. Guissani, *J. Chem. Phys.* **114**, 6720 (2001).

⁴⁷M. Neumann, *J. Chem. Phys.* **50**, 841 (1983).

⁴⁸K. T. Gillen, D. C. Douglass, and M. J. R. Hoch, *J. Chem. Phys.* **57**, 5117 (1972).

⁴⁹R. Mills, *J. Phys. Chem.* **77**, 685 (1973).

⁵⁰K. Krynicki, C. D. Green, and D. W. Sawyer, *Faraday Discuss. Chem. Soc.* **66**, 199 (1978).

⁵¹W. Wagner and A. Pruss, *J. Phys. Chem. Ref. Data* **31**, 387 (2002).

⁵²C. Vega, C. McBride, E. Sanz, and J. L. F. Abascal, *Phys. Chem. Chem. Phys.* **7**, 1450 (2005).

⁵³Y. Koyama, H. Tanaka, G. Gao, and X. C. Zeng, *J. Chem. Phys.* **121**, 7926 (2004).

⁵⁴O. Mishima and H. E. Stanley, *Nature (London)* **396**, 329 (1998).

⁵⁵R. Martoňák, D. Donadio, and M. Parrinello, *Phys. Rev. Lett.* **92**, 225702 (2004).

⁵⁶C. McBride, C. Vega, E. Sanz, and J. L. F. Abascal, *J. Chem. Phys.* **121**, 11907 (2004).